Hindawi
International Journal of Antennas and Propagation
Volume 2022, Article ID 4946518, 6 pages
https://doi.org/10.1155/2022/4946518

Research Article

Direction-of-Arrival Estimation in Time-Modulated Linear Arrays Based on the MT-BCS Approach

Qing-He Zhang[1,2] **En-Yu Zhang**[2] **and Shi-Hui Zhang**[2]

[1] *Hubei Key Laboratory of Intelligent Vision Based Monitoring for Hydroelectric Engineering, China Three Gorges University, Hubei, Yichang 443002, China*
[2] *College of Computer and Information Technology, China Three Gorges University, Hubei, Yichang 443002, China*

Correspondence should be addressed to Qing-He Zhang; zqh@ctgu.edu.cn

Received 27 September 2022; Revised 4 December 2022; Accepted 5 December 2022; Published 20 December 2022

Academic Editor: Sandeep Kumar Palaniswamy

This article proposes a novel approach for the estimation of the direction-of-arrival (DoA) of multiple signals impinging on time-modulated arrays (TMAs). The algorithm transforms DoA estimation into compressive sensing (BCS) formulation to tackle the sparse signal problem. Based on the voltage outputs of the TMAs at multiple times instants, a strategy using multitasks BCS (MT-BCS) is applied to recover the DoA and improve the accuracy. The comparison with the existing algorithms of DoA estimation in TMAs verifies the effectiveness and feasibility of the proposed method.

1. Introduction

Due to the sideband radiation characteristics, the time-modulated arrays (TMAs) are extensively used in various applications, such as future cognitive radio systems [1], electronic zero scanning [2], multibeam mode [3], wireless power transmission [4], and communication applications [5]. The direction-of-arrival (DoA) estimation has been an essential problem in array signal processing that has attracted significant attention and many studies have attempted to solve this problem based on the traditional phased array. On the contrary, few studies have been done on the DoA estimation in the TMAs. A method of DoA estimation based on the MUSIC algorithm in the TMAs was proposed [6], the sidebands were pointed in different directions, and the received data space could be formed through the corresponding received signals. In [7], the target of DoA could be recovered by comparing the carrier frequency of the echo signal with that of the transmitted signal. However, limited to the small number of snapshots, low signal-to-noise ratio (SNR), and correlated signals [8], the experimental results cannot meet the requirements.

Recently, compression sensing (CS) [9] has drawn significant attention due to its accuracy, computational efficiency, and robustness. Therefore, CS-based methods have already been applied to the DoA estimation of traditional antenna arrays [10].

The authors have previously estimated the DoA and bandwidth of unknown signals through the MT-BCS method based on the traditional phased array [11]. For the TMAs, few works have used the CS algorithm to estimate the azimuth information of the target signals. In [8], a weighted L1-norm with singular value decomposition operation (W-L1-SVD) method has been proposed for the DoA estimation in TMLA. Compared with the MUSIC algorithm, although the W-L1-SVD algorithm is improved and enhances the sparsity of the reconstructed coefficient vector, it is inefficient.

To overcome the above-mentioned drawbacks and satisfy the need for accurate and efficient estimation, this article provides a novel and effective approach based on MT-BCS for the DoA estimation in TMLA. The proposed algorithm based on Laplace prior [12] is used to recover the DoA in TMLA with a unidirectional phase center motion (UPCM) scheme [6], and it can perfectly cope with coherent signals.

The numerical results show that the proposed method has better estimation accuracy and efficiency compared with the MUSIC, L1-SVD, and W-L1-SVD methods.

Notations, vectors, and matrices are denoted with lowercase and capital letters in bold, respectively. The operators $(\cdot)^T$, $(\cdot)^H$, and $(\cdot)^{-1}$ represent transpose, Hermitian transpose, and inverse, respectively. ⊗ denotes the Kronecker product. I_a is an $a \times a$ identity matrix and $0_{a\times b}$ is an $a \times b$ zero matrix. di ag{·} denotes the diagonalization operation. Re{·} and Im{·} return the real and the imaginary parts of a variable, respectively.

2. Model of the TMLA with UPCM Scheme

Consider an isotropic TMLA consisting of N-element equidistant and narrowband far-field signals with the same carrier frequency f_0. Array elements are numbered 1 to N from left to right. First, the leftmost $M\,(M < N)$ elements open a time step τ, which is controlled as follows [6]:

$$\tau = \frac{T_p}{(N - M + 1)}, \tag{1}$$

where T_p is the time modulation period. The array factor of TMLAs is expressed as follows:

$$y(t) = \sum_{n=1}^{M} U_n(t) \cdot \sum_{k=1}^{K} s_k(t) \cdot e^{j(n-1)\beta d \sin\theta_k} + \eta_n(t), \tag{2}$$

where $s_k(t)$ is the kth narrowband far-field signal, d is the array element spacing, $\beta = 2\pi f_0/c$, $\eta_n(t)$ is the additive Gaussian white noise, and $U_n(t)$ is the switching function of the off time of the nth element. Due to the fact that high-speed RF switches periodically switch on and off according to a specific time sequence to realize the time modulation in TMAs, the received signals in some channels are forced to be zero during a certain time interval within one modulation period, which will deteriorate or invalidate conventional DoA estimation algorithms. Several strategies have been proposed to solve this problem, M. Pesavento, A. Gershman, and M. Haardt proposed the unitary root-MUSIC approach. M. Haardt and J. A. Nossek proposed a unitary ESPRIT approach. A novel approach for estimating DoAs in TMLAs with a unidirectional phase center motion (UPCM) scheme is proposed in this paper. With the UPCM scheme, the beams at different sidebands in TMLAs are capable of pointing in different directions [13], and the corresponding received signals can be used to compose a received data space [14]. Therefore, the UPCM scheme has been adopted in this article. According to the UPCM scheme, $U_n(t)$ is defined as follows [6]:

$$U_n(t) = \begin{cases} 1, & \mu_1\tau \le t \le \mu_2\tau, \\ 0, & \text{otherwise,} \end{cases} \tag{3}$$

where

$$\mu_1 = \begin{cases} 0, & n \le M, \\ n - M, & \text{otherwise,} \end{cases} \qquad \mu_2 = \begin{cases} n, & n \le N - M + 1, \\ N - M + 1, & \text{otherwise.} \end{cases} \tag{4}$$

To explain in detail, an example of a TMLA with $N = 24$ and $M = 2$ is shown in Figure 1. Since $U_n(t)$ is a periodic function of time, the spatial and frequency responses of (1) can be obtained by decomposing it into Fourier series, and each frequency component has a frequency of $f_0 + q/T_p\,(q = 0, \pm 1, \pm 2, \ldots \pm \infty)$. The Fourier component of qth order can be written as follows:

$$y_q(t) = \sum_{n=1}^{N}\sum_{k=1}^{K} b_{q,n} \cdot s_k(t) \cdot e^{j(n-1)\beta d \sin\theta_k} + \eta_n'(t), \tag{5}$$

where $\eta_n'(t)$ is the additive noise of the qth sideband and $b_{q,n}$ is the complex excitation of the qth-order sideband of the nth element and is expressed as follows [6]:

$$\begin{aligned} b_{q,n} &= \frac{1}{T_p}\int_{\mu_1\tau}^{\mu_2\tau} U_n(t) \cdot e^{-j2\pi q f_p t}\mathrm{d}t \\ &= f_p(\mu_2 - \mu_1)\tau \cdot \sin c\left[\pi q f_p(\mu_2 - \mu_1)\tau\right] \cdot e^{-j\pi q f_p(\mu_2+\mu_1)\tau}, \end{aligned} \tag{6}$$

where $f_p = 1/T_p$, $\sin cx = \sin x/x$. Assuming the number of maximum orders sidebands is Q. Then, the received signal can be expressed as follows:

$$Y = \left[y_{-Q}(t) y_{-Q+1}(t) \ldots\ y_Q(t)\right]^{\mathrm{T}} = \mathrm{B}\Phi(\theta)\mathrm{S} + \Theta(t), \tag{7}$$

where $\mathrm{B} = \left\{b_{q,n}\right\} \in \mathbb{C}^{N\times(2Q+1)}$, $\Phi(\theta) = [\phi_1(\theta)\phi_2(\theta)\ldots \phi_K(\theta)]$ is the array flow matrix, $\phi_k(t) = [1\ e^{j\beta d \sin\theta_k} \ldots e^{j(N-1)\beta d \sin\theta_k}]^{\mathrm{T}}$, $\mathrm{S} = [s_1(t)s_2(t)\ldots s_K(t)]^{\mathrm{T}}$ are the incident signals and $\Theta(t) = [\eta_1'(t)\eta_2'(t)\ldots\eta_N'(t)]^{\mathrm{T}}$ is the noise vector. Based on the above analysis, Section 3 introduces the DoA estimation method in TMLAs with the UPCM scheme.

3. DoA Estimation Based on MT-BCS

3.1. CS Model in TMLA. Assuming the entire space can be evenly divided into $(\theta_1, \theta_2, \ldots, \theta_I)$, and there are potential signals in each possible direction $\theta_i\,(i = 1, 2, \ldots, I, I \gg K)$, an overcomplete basis matrix $\mathrm{A}(\theta) = [\phi_1(\theta)\phi_2(\theta)\ldots\phi_I(\theta)]$ and a sparse signal vector $\mathrm{S} = [S_1(t)S_2(t)\ldots S_I(t)]^{\mathrm{T}}$ can be constructed accordingly. Considering that the signal vector S is K-sparse, (7) can be written as follows:

$$\mathrm{Y} = \mathrm{BA}(\theta)S + \Theta(t), \tag{8}$$

where $A(\theta)$ is the array flow pattern matrix and $\mathrm{BA}(\theta)$ is the $(2Q + 1)\times I$ measurement matrix in compressed sensing, where $I \gg 2Q + 1$.

Using the received data Y, a sparse reconstruction model of DoA estimation based on CS is defined as follows:

$$\hat{s} = \min \|\bar{s}\|_0 \ \text{s.t.}\ \|\mathrm{Y} - \mathrm{BA}(\theta)S\| \le \varepsilon, \tag{9}$$

where ε is the noise level parameter and $\|*\|_p$ is l_p-norm.

3.2. MT-BCS Model. The MT-BCS model is expressed as follows:

$$\mathrm{Y}_l = \mathrm{BA}(\theta)\mathrm{S}_l + \Theta_l(t), l = 1, 2, \ldots L, \tag{10}$$

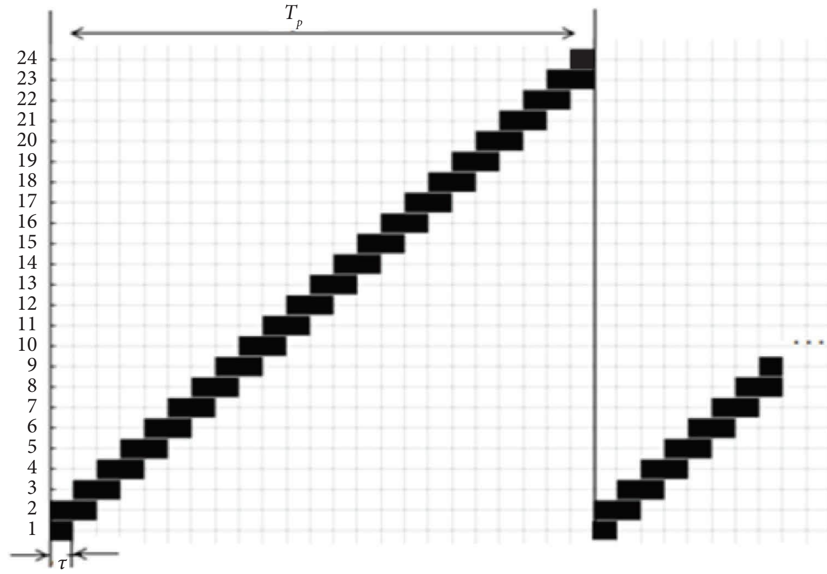

Figure 1: Time sequences of a 24-element TMLA with $M = 2$.

where L is the number of snapshots. The sparse signal vector is determined as follows:

$$\hat{s}_{\mathrm{MT-BCS}} = \frac{1}{L}\sum_{l=1}^{L}\left\{\arg\left[\max_{\bar{S}_l} p_r\left(|\wedge S_l, \gamma | \mathrm{Y}_l\right)\right]\right\}, \tag{11}$$

where $\hat{S}_l, l = 1, 2, \ldots L$ associates the hyperparameter vectors of different snapshots through appropriate "sharing." p_r is the prior probability function. The best values of the signal hyperparameter vector γ are computed through the following RVM formula [11]:

$$L^{MT-BCS}(\gamma) = -\frac{1}{2}\sum_{l=1}^{L}\left\{\log\left(\left|C_{\mathrm{MT-BCS}}\right|\right) + (I + 2\psi_1)\cdot\log\left[\mathrm{Y}_l^{\mathrm{T}}\left(C_{\mathrm{MT-BCS}}\right)\mathrm{Y}_l + 2\psi_2\right]\right\}. \tag{12}$$

With

$$\begin{aligned} C_{\mathrm{MT-BCS}} &\triangleq I + \hat{A}(\theta)\mathrm{diag}(\gamma)^{-1}\hat{A}(\theta)^{\mathrm{T}}, \\ \hat{\mathrm{A}}(\theta) &= \begin{bmatrix} \mathrm{Re}\{A(\theta)\} & -\mathrm{Im}\{\mathrm{A}(\theta)\} \\ \mathrm{Im}\{A(\theta)\} & \mathrm{Re}\{A(\theta)\} \end{bmatrix}, \end{aligned} \tag{13}$$

where ψ_1, ψ_2 are the user-defined parameters, while Re$\{*\}$ and Im$\{*\}$ are the real and the imaginary parts, respectively. Finally, the solution estimated by the MT-BCS is equal to

$$\hat{s}_{\mathrm{MT-BCS}} = \frac{1}{L}\left(\sum_{l=1}^{L}\left\{\left[\mathrm{A}(\theta)^{\mathrm{T}}\hat{\mathrm{A}}(\theta) + \mathrm{diag}\left(\gamma_{\mathrm{MT-BCS}}\right)\right]^{-1}\hat{\mathrm{A}}(\theta)^{\mathrm{T}}\mathrm{Y}_l\right)\right). \tag{14}$$

4. Numerical Results

In this section, the proposed MT-BCS algorithm is used for DoA estimation in TMLA with 24 elements UPCM timing sequence and compared with the MUSIC and SVD algorithms. The following experiments are conducted to determine the appropriate value of Q. The root-mean-square error (RMSE) is used to assess different DoA estimation methods. The RMSE is defined as follows:

$$\mathrm{RMSE} = \frac{1}{K}\sum_{k=1}^{K}\sqrt{\frac{1}{T}\sum_{t=1}^{T}\left(\hat{\theta}_k(t) - \theta_k\right)^2}, \tag{15}$$

where $\hat{\theta}_k(t)$ is the estimate of θ_k in the t−th experiment and t is the number of Monte Carlo runs. The statistical results of RMSE are obtained through an average of $T = 100$ simulations.

Suppose that there are three uncorrelated signals with random codes and equal power, arriving from $\theta_1 = -8^0, \theta_2 = 0^0$ and $\theta_3 = 14^0$. To select the appropriate value of Q, Figure 2 shows the RMSE of different methods versus the Q with 15 dB SNR and 50 snapshots. It can be seen that Q has no significant impact on the RMSEs of the three algorithms, and the proposed MT-BCS is stable after $Q \geq 5$. In the MUSIC algorithm, the RMSE decreases with the increase in Q and stabilizes after $Q \geq 8$. Thus, $Q = 8$ is adopted in the following study.

For the uncorrelated sources, the RMSEs in different SNRs and snapshots are shown in Figures 3 and 4, respectively. Figure 5 shows the corresponding spatial spectrums at $L = 50$ and SNR $= 15$ dB.

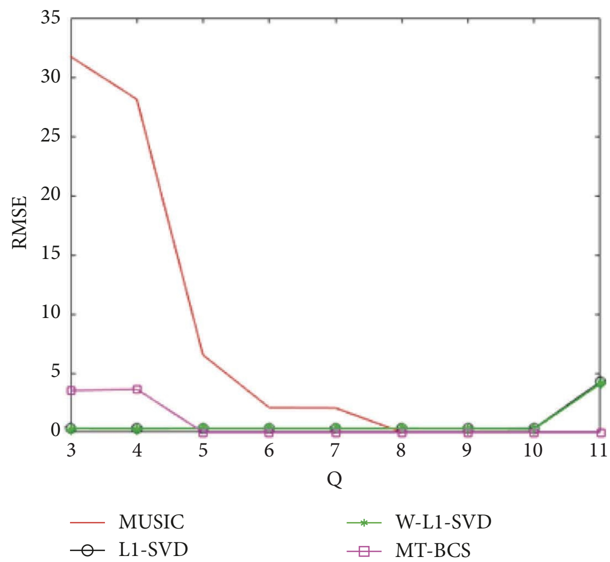

Figure 2: RMSEs versus Q at $L = 50$, $\mathrm{SNR} = 15$ dB for different methods.

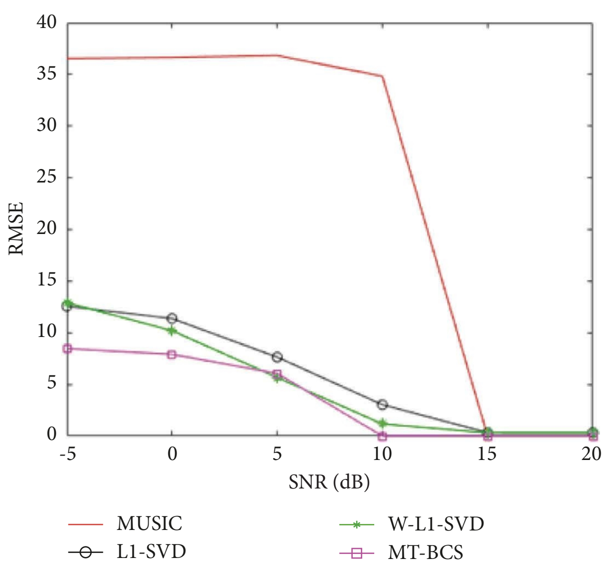

Figure 3: RMSEs for uncorrelated sources versus different SNR with $L = 50$ for different methods.

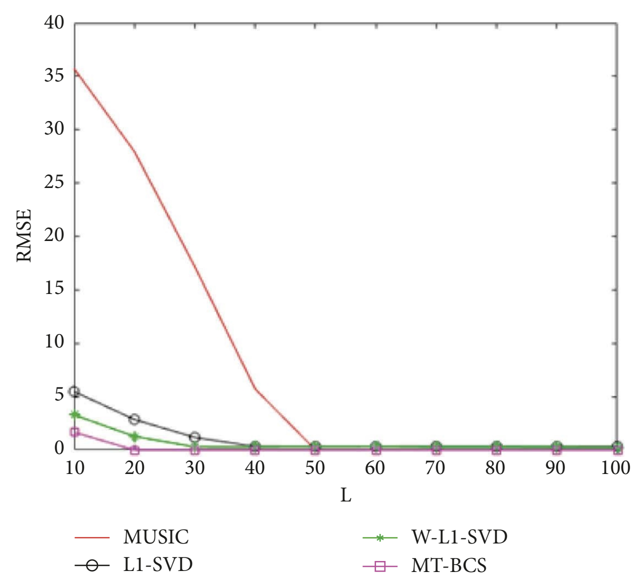

Figure 4: RMSEs for uncorrelated sources versus different snapshots with $\mathrm{SNR} = 15$ dB for different methods.

The results indicate that the proposed method has superior performance, especially under the circumstance of the low SNR, as well as the small number of snapshots. According to the results shown in Figure 3, the proposed method can estimate DoA accurately with a very small error when the SNR is greater than 10 dB. It can be seen from Figure 5 that the MUSIC algorithm has sharper spectral peaks while having large false peaks, and if the parameters are inappropriate, the estimation results turn inaccurate, according to the results shown in Figures 3 and 4. The false peaks of the W-L1-SVD algorithm are significantly suppressed, and the spectral peaks of the W-L1-SVD algorithm are sharper than those of the L1-SVD algorithm. The proposed algorithm does not need to consider false peaks because it mainly estimates the amplitude of the angle with strong signal energy, such as shown in Figure 5(d). The uninterested estimated magnitude of DoA is smaller.

Figure 6 shows the RMSEs of different algorithms for correlated sources. The results show that the proposed method has better estimation results than the other three algorithms even in the correlated source.

Table 1 compares the computational times of four different algorithms in the same scenario. The time consumption of the two SVD algorithms is close. The time consumption of the proposed method is longer than that of the MUSIC method but less than that of the two SVD methods. It shows that the proposed MT-BCS method has better efficiency than the SVD-based algorithms.

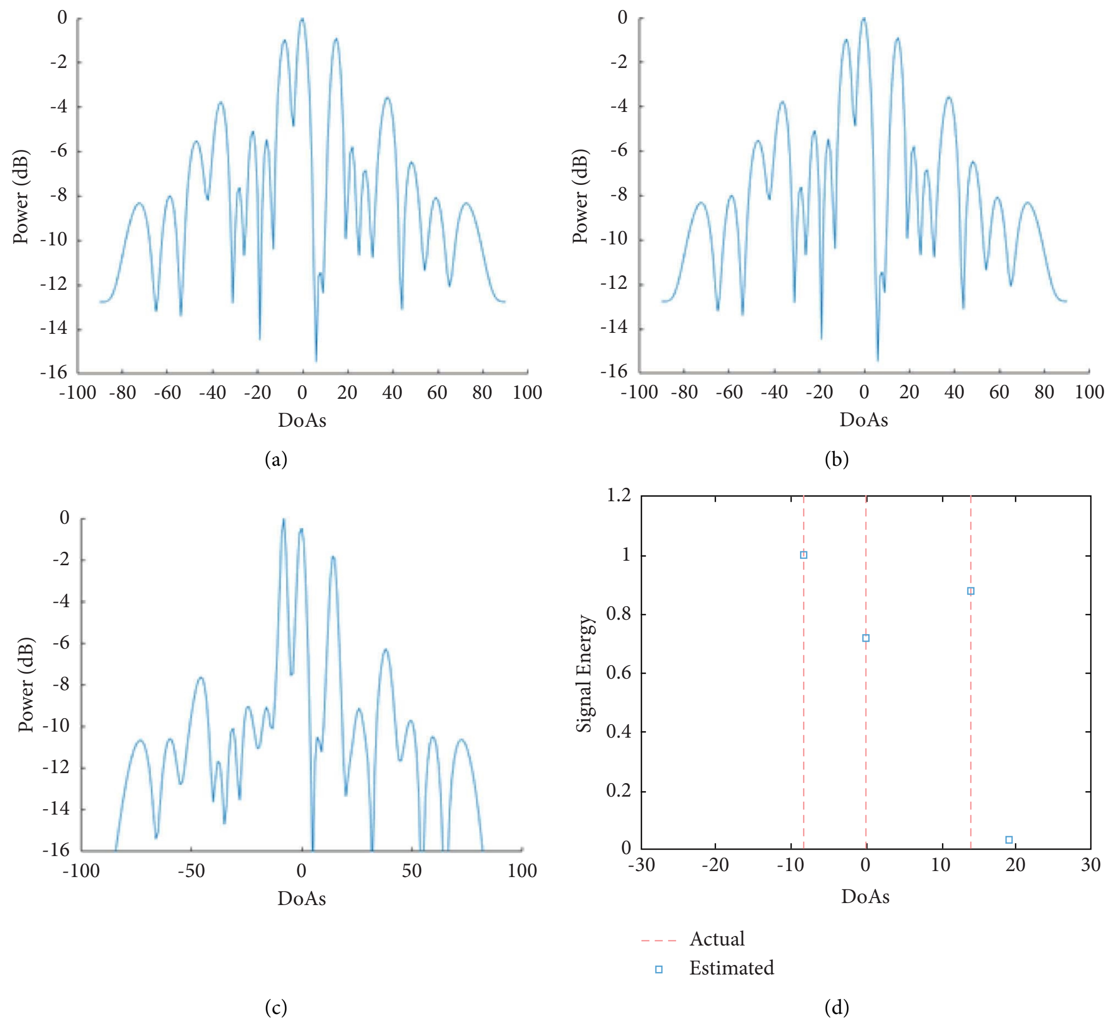

Figure 5: Spatial spectrums of the uncorrelated sources for different methods. (a) MUSIC. (b) L1-SVD. (c) W-L1-SVD. (d) MT-BCS.

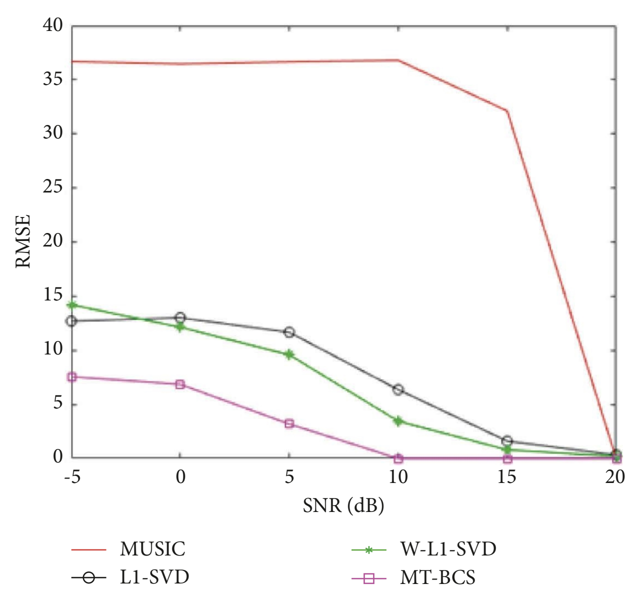

Figure 6: RMSEs versus SNR with 50 snapshots for correlated sources for different methods.

Table 1: Computational times of different algorithms.

Algorithm	MUSIC	L1-SVD	W-l_1-SVD	MT-BCS
Time (s)	0.010	3.810	3.726	0.116

5. Conclusion

This paper proposes a novel and effective method called MT-BCS to deal with the direction-of-arrival estimation problem in time-modulated linear arrays. The simulation results show that the proposed method can obtain a more accurate DoA estimation compared with the MUSIC and SVD algorithms, even in the case of low SNR, small snapshots, and signal coherence. Moreover, the computational time of the proposed algorithm is also less than the SVD-based algorithms.

Data Availability

The data are available upon request from the corresponding authors.

Conflicts of Interest

The authors declare that they have no conflicts of interest.

References

[1] P. Rocca, Q. Zhu, E. T. Bekele, S. Yang, and A. Massa, "4D arrays as enabling technology for cognitive radio systems," *IEEE Transactions on Antennas and Propagation*, vol. 62, no. 3, pp. 1102–1116, 2014.

[2] A. Tennant and B. Chambers, "A two-element time-modulated array with direction-finding properties," *IEEE Antennas and Wireless Propagation Letters*, vol. 6, no. 3, pp. 64-65, 2007.

[3] L. Poli, P. Rocca, G. Oliveri, and A. Massa, "Harmonic beamforming in time-modulated linear arrays," *IEEE Transactions on Antennas and Propagation*, vol. 59, no. 7, pp. 2538–2545, 2011.

[4] D. Masotti, A. Costanzo, M. Del Prete, and V. Rizzoli, "Time-modulation of linear arrays for real-time reconfigurable wireless power transmission," *IEEE Transactions on Microwave Theory and Techniques*, vol. 64, no. 2, pp. 331–324, 2016.

[5] Y. Yashchyshyn, K. Derzakowski, P. R. Bajurko, J. Marczewski, and S. Kozlowski, "Time-modulated reconfigurable antenna based on integrated S-PIN diodes for mm-wave communication systems," *IEEE Transactions on Antennas and Propagation*, vol. 63, no. 9, pp. 4121–4131, 2015.

[6] G. Li, S. Yang, and Z. Nie, "Direction of arrival estimation in time modulated linear arrays with unidirectional phase center motion," *IEEE Transactions on Antennas and Propagation*, vol. 58, no. 4, pp. 1105–1111, 2010.

[7] D. Ni, S. Yang, Y. Chen, and F. Yang, "Direction finding based on TMAs with reconfigurable angle-searching range and bearing accuracy," *Electronics Letters*, vol. 53, no. 3, pp. 130–132, 2017.

[8] W. T. Li, Y. J. Lei, and X. W. Shi, "DOA estimation of time-modulated linear array based on sparse signal recovery," *IEEE Antennas and Wireless Propagation Letters*, vol. 16, no. 6, pp. 2336–2340, 2017.

[9] E. Candes and M. Wakin, "An introduction to compressive sampling," *IEEE Signal Processing Magazine*, vol. 25, no. 2, pp. 21–30, 2008.

[10] M. Carlin, P. Rocca, G. Oliveri, F. Viani, and A. Massa, "Directions-of-arrival estimation through bayesian compressive sensing strategies," *IEEE Transactions on Antennas and Propagation*, vol. 61, no. 7, pp. 3828–3838, 2013.

[11] S. H. Zhang, Q. H. Zhang, L. P. Shi, C. Yi, and G. X. Liu, "Mt-bcs-based doa and bandwidth estimation of unknown signals through multiple snapshots data," *International Journal of Antennas and Propagation*, vol. 2020, no. 4, Article ID 6179280, 7 pages, 2020.

[12] S. D. Babacan, R. Molina, and A. K. Katsaggelos, "Bayesian compressive sensing using laplace priors," *IEEE Transactions on Image Processing*, vol. 19, no. 1, pp. 53–63, 2010.

[13] S. Ji, Y. Xue, and L. Carin, "Bayesian compressive sensing," *IEEE Transactions on Signal Processing*, vol. 56, no. 6, pp. 2346–2356, 2008.

[14] O. Kramer, T. Djerafi, and K. Wu, "Vertically multilayer-stacked yagi antenna with single and dual polarizations," *IEEE Transactions on Antennas and propagation*, vol. 58, no. 4, pp. 1022–1030, 2010.